European Journal of Human Movement

Original Research

Estimation of an elite road cyclist resistive forces and performance wearing standard and aero helmets: an analytical procedure and numerical simulations approach

Pedro Forte [1,2,3*], Daniel Marinho [3,4], Tiago M Barbosa[2,3], Jorge E Morais[2,3,4]

[1] Douro Higher Institute of Educational Sciences, Penafiel, Portugal.
[2] Instituto Politécnico de Bragança, Bragança, Portugal.
[3] Research Center in Sports Health and Human Development, Covilhã, Portugal.
[4] University of Beira Interior, Covilhã, Portugal.

* Correspondence: (author initials) peromiguel.forte@iscedouro.pt ORCID ID nº 0000-0003-0184-6780

Received: 20/09/2020; Accepted: 22/04/2021; Published: 31/06/2021

Abstract: The aim of this study was to assess and compare by numerical simulations and analytical models the resistive forces, mechanical power, energy cost and velocity using two different types of road helmets (standard vs aero road helmet). An elite cyclist was scanned on the racing bicycle, wearing his competition gear and helmets. Numerical simulations by Computational Fluid Dynamics were carried-out at 11.11 m/s (40 km/h) and 20.83 m/s (75 km/h) to extract the drag force. The mechanical power and energy cost were estimated by analytical procedures. The drag forces were between 9.93 N and 66.96 N across the selected speeds and helmets. The power to overcome drag were 182.19 W and 1121.40 W. The total power lower and higher values were 271.05 W and 1558.02 W. The energy cost estimation was between 106.89 J/m and 381.40 J/m across the different speeds and helmets. The standard helmet imposed higher drag and demanded more power.

Keywords: cycling; helmets; cfd; power; energy cost

1. Introduction

In time-based sports, final race time (i.e. acceleration and therefore velocity) depends on the balance between thrust (propulsive force: Fprop; and resistance: Fresist):

$$a = \frac{(F_{prop} - F_{resist})}{m} \quad (1)$$

Drag and rolling resistance are the main resistive forces in cycling with opposite direction of the movement. The cycling fraternity seeks to find out strategies and equipment that may improve the riders' race time (Candau et al., 1999). The Cyclists adopt different positions during a race and wear specific gear (Beaumont, Taiar, Polidori, Trenchard, & Grappe, 2018). The road profile and expected average speed or pace, set the cyclists' positions and equipment to worn. During a road race or in a stage, cyclists choose to adopt either one of these two main positions: (i) upright position; or (ii) "elbows" position (Blocken, 2018b).

To reach a target velocity (and as such an estimated time of arrival), energy is required to overcome the resistive forces:

$$v = \sqrt{\frac{2.\varepsilon_{kin}}{m}} \tag{2}$$

Where, v is velocity, ε is the kinetic energy and m is the mass. Hence, velocity is dependent on the energy delivered by the rider (εin) and the energy lost (εloss) by the bicycle-cyclist system. Cyclists aim to reach the maximal mean velocity and delivering the least energy at a given pace (efficiency) (Lucia, Earnest, & Arribas, 2003):

$$v = \sqrt{\frac{2(\varepsilon_{in} - \varepsilon_{loss})}{m}} \tag{3}$$

The rolling resistance is possible to minimize by the bicycle-cyclist system mass reduction (Grappe et al., 1999). Bicycles made of light materials such as carbon and/or aluminium fibres and high-pressure tires are recommended to minimize rolling resistance (Ryschon & Stray-Gundersen, 1993). The cyclist's mass, tyres' pressure, casing construction, and the gradient and texture of the riding surface also influence the rolling resistance (Candau et al., 1999; Barelle, Chabroux, & Favier, 2010; Martin et al., 1998). Hence, bicycle-cyclist system mass can be reduced by changing the bicycle's materials and/or the cyclist's body mass.

The drag represents about 90% of the resistive forces and the cyclist's body causes 60%-70% of total drag (Defraeye, Blocken, Koninckx, Hespel & Carmeliet, 2010a; Kyle & Burke, 1984; Gross, Kyle & Malewicki, 1983). Several authors have reported the drag effects in different body positions (Defraeye et al., 2010a; Grappe, Candau, Belli & Rouillon, 1997). The positions with lower projected surface area are also the ones submitting less drag (Defraeye et al., 2010a; Grappe et al., 1997). Among the different positions that cyclists can adopt, the time-trial position imposes less drag reducing the surface area (Defraeye et al., 2010a). Indeed, reducing the surface area also explains the drafting phenomenon in pelotons; where cyclists can save about 40% of energy cost when compared to an isolated cyclist (Blocken et al., 2018). So, it is common to see cyclists adopting specific positions while riding in straight lines, such as the "elbows" position (due to the similarities with the time-trial position, regarding the lower surface area) (Blocken, 2018b).

Drag force is possible to split into pressure and viscous drag components. Viscous drag results from the interaction between the bicycle-cyclist surface and the fluid (Debraux, Grappe, Manolova & Bertucci, 2011). In cycling, the dragged fluid (air) to the system is the viscous drag (Debraux et al., 2011; Edwards & Byrnes, 2007). The first layer of dragged air will make a following layer attach to itself and this phenomenon will occur in the nearby layers (Debraux et al., 2011; Schlichting & Gersten, 2016). The surface roughness will be determinant to the viscous drag (Debraux et al., 2011; Edwards & Byrnes, 2007). Pressure drag has the highest contribution to total drag in cycling (Grappe et al., 1999; Lukes, Chin & Haake, 2005; Kyle & Burke, 1984). The pressure drag results from the fluid distortion in the rear edges and the pressure differences between the bicycle-cyclist system' front and back boundaries (Schlichting & Gersten, 2016). The body shape is determinant for the pressure differences between the boundaries (Kennedy & Lampe, 2013; Debraux et al., 2011; Schlichting & Gersten, 2016; Burke, 2003; Chowdhury, 2012; Defraeye, Blocken, Koninckx, Hespel, & Carmeliet, 2010b; Kulfan, 2000).

Riders may wear different equipment with different features to minimize drag, such as helmets (Barelle et al., 2010; Beaumont et al., 2018). There are two main types of helmets: (i) standard and; (ii) aero road helmet. Air vents and protection characterize standard helmets; whereas, the aero road helmets are characterized by different tail lengths and reduced or no air vents to improve efficiency and aerodynamics (Beaumont et al., 2018; Brühwiler et al., 2006; Forte et al., 2017).

Recently, elite road cyclists have been using these "new" aero road helmets that are characterized by time-trial features. These have larger areas without air vents. It may be speculated that such specifications were developed to minimize drag and improve efficiency, as it happens in time-trial helmets (Beaumont et al., 2018). However, it is yet unclear what is the effect of these new type of helmets on a rider's aerodynamics, mechanical power, energy cost and estimated time of arrival (ETA).

The aerodynamics can be assessed by analytical procedures, experimental techniques (coasting down or wind tunnel testing) and numerical simulations (by computational fluid dynamics) (Debraux et al., 2011; Forte, Barbosa, & Marinho, 2015). The analytical procedures require a set of assumptions such as drag coefficient and air density. The numerical simulations by computer fluid dynamics (CFD) allows assessing drag in specific and controlled conditions (Forte et al., 2015). This methodology allows determining the fluid flow behaviour and outputs such as pressure values, pressure, viscous and total drag and coefficient of drag (Defraeye et al., 2010a; Forte, Marinho, Morais, Morouço, & Barbosa, 2018a). Then, it is possible to estimate cyclists' mechanical power and energy cost with a reliable method (Grappe et al., 1997; Martin et al., 1998; Forte et al., 2018b).

The aim of this study was to assess and compare the resistive forces, mechanical power, energy cost and performance (velocity) wearing two types of road helmets (standard vs. aero road helmet) by numerical simulations and analytical models. It was hypothesized that: (i) the drag will be lower in the aero road helmet; (ii) the mechanical power and energy cost will be lower in the aero road helmet; (iii) the estimated arrival time (velocity) will be better wearing aero road helmets.

2. Materials and Methods

The Methods section should be limited to material available at the time of the study design, whereas information obtained during the study should appear in the Results section. The Methods section should include a description of the design, subject information (including a statement that institutional review board approval was granted, in the spirit of the Helsinki Declaration), interventions, outcome measures, and statistical analyses.

Subjects — An elite level road cyclist, racing regularly at national level events volunteered to take part in this study. The bicycle-cyclist system mass was 62 kg (cyclist: 55.0 kg of body mass and 1.76 m of height). All procedures were in accordance to the Helsinki Declaration regarding human research and a written consent was obtained beforehand.

Scanning the model —The cyclist was scanned on his racing bicycle, wearing competition gear and each of the two helmets. The scans were made in the same elbows position wearing either a standard helmet (Figure 1a; Giant, Rev Helmet) or an aero road helmet (Figure 1b; Giant, Pursuit Helmet) (figure 1). During the procedure, the participant was asked to maintain his position and body alignment. The researcher responsible for scanning the model changed his helmet. The Rev Helmet type directs the incoming air from the front and side to the back channels; whereas the Pursuit Helmet reduces the ventilation (having only two ventilation channels: front and back) for a similar time-trial helmet's aerodynamic profile. The Rev Helmet weights 280 g; controversy, the Pursuit Helmet weights 250 g. The helmets were made with resistant polycarbonate with foam in the inside part.

The scanning was made by a Sense 3D scanner (3D Systems, Inc., Canada) and saved in the Sense Software (Sense, 3D Systems, Inc., Canada). Upon that, Geomagic studio (3D Systems, USA) was used for geometric editing in post processing. The models were meshed, smoothed, clean self-intersections, spikes and non-manifold edges. Then the objects were converted into CAD models (Forte et al., 2018) (figure 2).

Boundary conditions — The models were imported into Ansys Workbench software (Ansys Fluent 16.0, Ansys Inc., Pennsylvania,

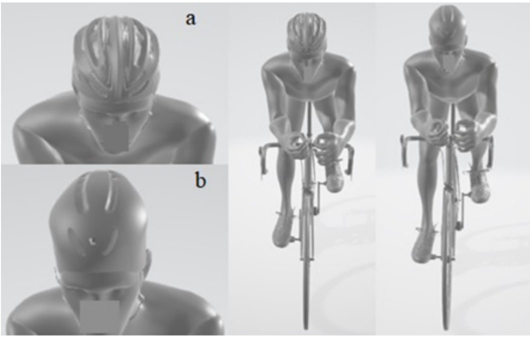

Figure 1. Standard (a) and aero road (b) helmet at time-trial position (right picture: the geometries figures were retrieved with different zoom levels).

USA). Following that, the boundary dimensions were created in the geometry module. A three-dimensional domain was created around the cyclist. The domain was meshed to represent the fluid flow in the opposite direction to the cyclist (figure 2). The domain had 7 m of length, 2.5 m of width and 2.5 m of height. Then, the meshing module (Ansys Mesh, Ansys Inc., Pennsylvania, USA) computed the greed/mesh around the CAD models with 42 million of prismatic and tetrahedral elements. The cyclist was placed at 2.5 meters of the inlet portion (Blocken et al., 2013).

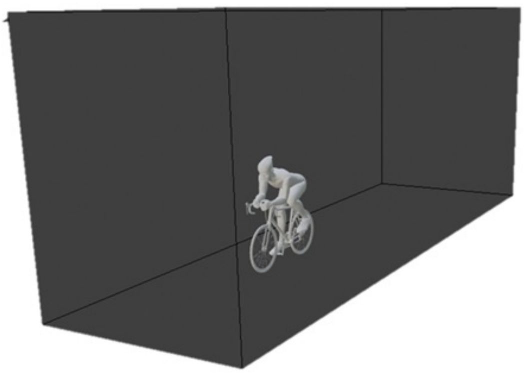

Figure 2. Three-dimensional domain around the cyclist with the aero helmet.

During a race, the mean speed is about 11.1 m/s (~40 km/h) (El Helou et al., 2010; Forte et al., 2020). However, during downhill events, a cyclist can reach a mean speed of 20.83 m/s (~75 km/h) (Dorel et al., 2005; Forte et al., 2020). The velocity was set at the inlet portion of the enclosure surface (-z direction) at the steady velocities of 11.1 and 20.83 m/s (~40 km/h and ~75 km/h, respectively). These speeds were then selected to better understand the resistive forces at the mean stage speed and sprinting or downhill events. The turbulence intensity was assumed as 1×10^{-6}%. This procedure was carried out for the geometries with a standard helmet and with the aero road helmet (aero helmet). The bicycle-cyclist system was orientated to the negative direction of z axis. The surface of the bicycle-cyclist system was established as zero roughness non-slip wall and scalable wall functions were assigned.

Numerical simulations — The Fluent CFD code (Ansys Fluent 16.0, Ansys Inc., Pennsylvania, USA) run the Reynolds-averaged Navier–Stokes (RANS) equations. The RANS equations convert instantaneous values into means. Fluent CFD code (Ansys Fluent 16.0, Ansys Inc., Pennsylvania, USA.) allowed solving these equations using the finite volume approach. Realizable k-e was the selected turbulence model. Velocity histograms are very similar to the standard k-e, RST and RNG k-e models (Aroussi et al., 2001). The realizable k-epsilon presents a higher computation economy (Aroussi et al., 2001). The standard wall function was selected for this simulation.

The SIMPLE algorithm was used for pressure–velocity coupling. The pressure interpolation and the convection and viscous terms of the governing equations discretization schemes were defined as second. The least-squares cell-based method computed the gradients. Pressure and momentum were defined as second order and second order upwind and the turbulent kinetic energy and turbulent dissipation rate as first order upwind. The convergence occurred automatically by the Ansys Fluent 16.0 (Ansys Fluent 16.0, Ansys Inc., Pennsylvania, USA) before 1,404 interactions.

Outcomes —

Drag force — After the numerical simulations converging, outputs such as viscous, pressure, total drag and coefficient of drag are possible to obtain. Ansys Fluent Software (Ansys Fluent 16.0, Ansys Inc., Pennsylvania, USA) computed the surface area. Then, the AC_d was computed.

Total aerodynamic drag (F_d) and frontal surface area were retrieved from Fluent code (Ansys Fluent 16.0, Ansys Inc., Pennsylvania, USA) software. To compute the drag force, equation (4) was used:

$$F_d = \frac{1}{2}\rho A C_d v^2 \tag{4}$$

Where, F_d is the drag force, C_d represents the drag coefficient, v the velocity, A the surface area and ϱ is the air density (1.292 kg/m^3).

Mechanical Power and Energy Cost — The power to overcome drag (equation 5) was calculated at the selected speeds as (Candau et al., 1999):

$$P_d = F_d . v_x \tag{5}$$

Where P_d is the power to overcome drag, F_d the drag force and v_x the horizontal velocity.

Knowing drag and rolling resistance, equation 6 enables the assessing of the energy cost (i.e., energy expenditure per unit of distance) (Candau et al., 1999).

$$C = \frac{CR.m.g + \frac{\rho}{2}.A.C_d.v^2}{n} \tag{6}$$

In equation 6, C is the energy cost, CR is the rolling coefficient, m the body mass of the bicycle-cyclist system, g the gravitational acceleration, v the mean velocity over the race, ϱ the air density, A is the surface area and C_d the drag coefficient and η the gross efficiency. The assumed gross efficiency of cyclists is 20% (Bertucci, Betik, Duc, & Grappe, 2012) and CR 0.00368 (Candau et al., 1999).

Total Net Power (PNET, equation 11) results from the sum of power to overcome drag (equation 2), power of bearing friction (PWB, equation 7), power of the rolling resistance (PRR, equation 8), Changes in Potential Energy (PPE, equation 9) and changes in kinetic energy (equation 10) (Martin et al., 1998).

$$P_{WB} = v\,(91 + 87v)10^{-3} \tag{7}$$

$$P_{RR} = CR.m.v.g \tag{8}$$

$$P_{PE} = v.m.v.g \tag{9}$$

$$P_{KE} = \frac{\Delta KE}{\Delta t} = \frac{1}{2}\left(m + \frac{I}{r^2}\right)\left(V_f - V_i\right)/(t_i - t_f) \tag{10}$$

$$P_{NET} = Pd + P_{WB} + P_{RR} + P_{PE} + P_{KE} \tag{11}$$

$$P_{TOT} = (Pd + P_{WB} + P_{RR} + P_{PE} + P_{KE})/E_c \tag{12}$$

Thus, total NET power (PNET) and total power (PTOT) can be computed by equations 11 and 12. In equation 12, Ec is the chain efficiency factor and assumed as 0.976 (Martin et al., 1998).

Performance

Performance of each mechanical power and speed was estimated by estimated arrival time (ETA) by direct proportionality. ETA is given by:

$$ETA = \frac{d}{v} \tag{13}$$

3. Results

Drag force — The drag force ranged between 9.93 N and 66.96 N across the selected speeds (Figure 3). Effective area (ACd) ranged between 0.20 and 0.26 m^2. The largest magnitude was observed wearing the standard helmet for both speeds in comparison to the aero helmet. For the standard helmet, at 11.1 m/s and 20.83 m/s the total drag ranged between 19.67 N and 66.96 N. In the aero helmet, for the same speeds, drag ranged between 16.41 N and 53.84 N. At 11.1 m/s the difference in total drag between the normal and aero helmet was 17%. The viscous drag differences were 13% and the pressure drag difference was 20%. At 20.83 m/s the total drag difference between both helmets was 20%. The viscous drag and pressure drag was 17% and 23% lower, respectively, in the aero helmet.

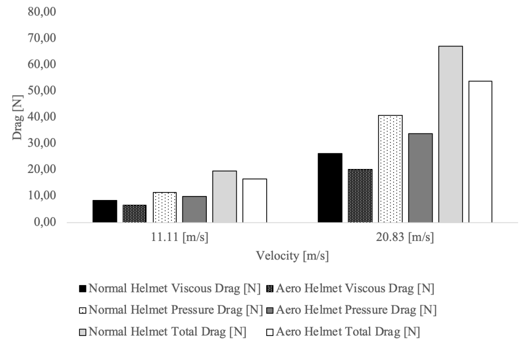

Figure 3. Total, viscous and pressure drag differences between a normal (Giant, Rev Helmet) and an aero (Alpina, Elexxion TT) helmet at 11.11 and 20.83 m/s.

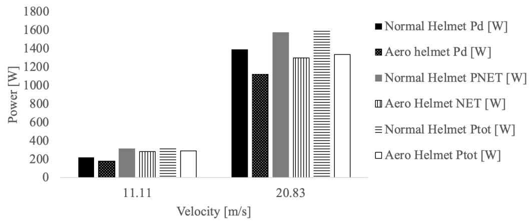

Figure 4. Power to overcome drag, net power and total power at different speeds and helmets.

Mechanical Power and Energy Cost — The power to overcome drag ranged between 182.19 W and 1121.40 W at 11.11 and 20.83 m/s (figure 4). For the normal helmet, the Pd was 218.37 W and 1394.87 W at 11.11 and 20.83 m/s, respectively. The aero helmet Pd was 182.19 W and 1121.40 W. At 11.11 m/s the aero helmet demanded 17% less power to overcome drag than the aero helmet. At 20.83 m/s, the aero helmet saves 20% less power to overcome drag. The PNET varied between 264.54 and 1520.62 W. The aero helmet encompassed 17% less at 20.83 m/s and 11% at 11.11 m/s. The Ptot went from 271.05 W to 1558.02 W and the aero helmet had less 17% Ptot at 20.83 m/s and 11% at 11.11 m/s in comparison to the normal helmet.

The power of bearing friction (PWB) was 1.73 W at 11.11 m/s and 20.83 m/s for both helmets. The power of rolling resistance (PRR), changes in potential energy (PPE) and power related to the changes in potential energy (PKE) were 24.82 and 46.58 W at 11.11 and 20.83 m/s in both helmets. The delivered power per body mass ranged (W/kg) between 4.37 W/kg and 21.52 W/kg at different speeds and helmets. The aero helmet had less 11% and 17% at 11.11 m/s and

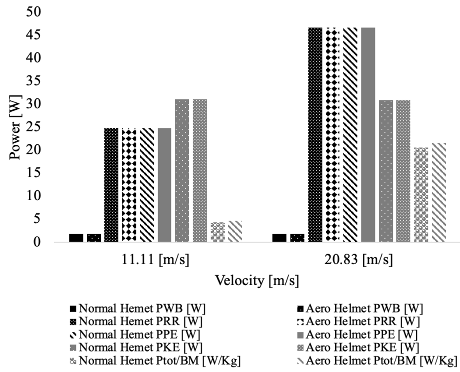

Figure 5. Power of bearing friction (PWB), Power of the rolling resistance (PRR), changes in Potential Energy (PPE), power related to the changes in potential energy (PKE) and Total Power by Body Mass (W/kg) at different speeds and helmets.

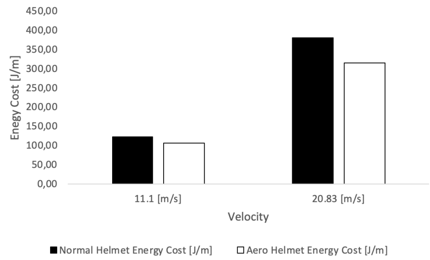

Figure 6. Energy cost at different speeds and helmets.

20.83m/s respectively, than the normal helmet (figure 5).

The cyclist energy cost estimation varied between 106.89 J/m and 381.40 J/m across the different speeds and helmets as presented in figure 6. The normal helmet presented an energy cost of 123.19 J/m and 381 J/m at 11.11 m/s and 20.83 m/s, respectively. The cyclist energy cost with an aero helmet ranged between 106.89 J/m and 315.75 J/m at 11.11 m/s and 20.83 m/s. At 11.11 m/s, the aero helmet imposed less 15% J/m; whereas, at 20.83 m/s, the energy cost difference between the normal and aero helmet was 21%.

Performance — Performance was measured by the estimated arrival time (ETA) (figure 7). Wearing a standard helmet, the cyclist had to deliver 327 W to reach 11.11 m/s; whereas with an aero helmet the subject needs to deliver 290 W. At 20.83 m/s, the subject had to impose higher power with a normal helmet (1614.35 W) in comparison to an aero helmet (1334.15 W). Wearing an aero helmet, for the same mechanical power as normal helmet, it is estimated that the cyclist reaches 12.51 m/s and 25.20 m/s. Overall, in 152 km at 327 and 1614.35 W, a cyclist with an aero helmet may save 1543.41 and 1265.42 s (Figure 7), about 18%.

4. Discussion

The aim of this study was to assess resistive forces, mechanical power and energy cost of a cyclist by numerical simulations and analytical models with different helmets and speeds on a "elbows" position. No research was found estimating the cyclists' mechanical power and energy cost by numerical simulations and analytical procedures wearing standard and aero road helmets on a "elbows" position. The main results were: (i) standard helmet imposed more drag than the aero road helmet at the different speeds; (ii) energy cost and mechanical power were higher wearing the standard helmet at the different speeds.

The drag force ranged between 9.93 N and 66.96 N at 11.11m/s (~ 40 km/h) and 20.83 m/s (~ 75 km/h) by numerical simulations. For the CFD analysis, air density of 1.292 kg/m^3 and a temperature of 15º C were assumed, being standard values reported in literature (Forte et al., 2018). Typically, cyclists had a mean speed of 40 km/h (11.11 m/s) at the Tour de France (El Helou et al., 2010). Speeds near 75 km/h (20.83 m/s) are typically reached in downhill stretches and sprinting (Dorel et al., 2005). Beaumont et al. (2018), reported an ACd between 0.134 m^2 and 0.142 m^2. However, the authors did not include the bicycle in the analysis. García-López et al. (2008) noted ACd values near 0.26 m^2. Moreover, Zdravkovic, Ashcroft, Chisholm, & Hicks (1996), reported that in the time-trial position ACd varies from 0.17 m^2 to 0.23 m^2. In our study, ACd ranged between 0.20 m^2 and 0.26 m^2. Cyclists adopt similar time trial positions while riding in straight lines to reduce the surface area and drag, such as the "elbows" position (Blocken, 2018b). The drag differences between helmets and speeds ranged from 17% to 23%. Beaumont et al. (2018) assessed the differences between three helmets by CFD. The authors reported that drag coefficient differed about 3.1%. Noteworthy, the drag coefficient was not used to assess the aerodynamic differences and, drag and drag coefficient varied with speed. Forte et al. (2016) reported that, the difference in drag between an angle of attack of 0º and 90º with a normal helmet at 5.5 m/s was 16%. The selected velocity was slower. However, the results seem to be aligned to our findings. In the present study, pressure drag accounted to 58-63% of total drag; whereas, viscous drag contribution ranged between 37% and 42%. In cycling, pressure drag is noted as the main contributor for total drag (Faria, Parker, & Faria, 2005) and, viscous drag is strongly dependent of the surface roughness. However, no study was yet found reporting viscous drag values by CFD. Overall, pressure drag was the main contributor for total drag.

The PWB was 1.73 W. The PRR, PPE and PKE ranged from 24.82 to 46.58 W. The delivered power per body mass went from 4.37 W/kg to 21.52 W/kg. Martin et al (1998) assessed the same variables by their model at mean speeds between 6.1m/s and 12.1 m/s. They reported a PWB between 1 and 2.1 W, PPE between 16.5 and 26.7 W, PRR from 18.2 to 29.4 W and, PKE ranged between 0.6 and 2.2 W. The delivered power per body mass ranged between 4.37 W/kg and 21.52 W/kg at different speeds and helmets, at 11.11m/s the power per body mass ranged between 4.37 and 4.69 W/Kg. These values seem to be in agreement with literature at similar speeds. Over an entire race or stage, trained cyclists can deliver a power per body weight ranging between 4 and 6 W/kg. However, during 5 s, world-class cyclists can achieve 25.18 W/kg. These values are near the delivered power at 20.83 m/s, reached mainly in downhill or sprinting events (Schenau, de Koning & de Groot, 1994).

The mechanical power was estimated considering the analytical model reported by Martin et al. (1998). The mechanical power ranged between 290.01 W and 1614.35 W at the different speeds and helmets. The power to overcome drag ranged between 182.19 W and 1394.97 W. In laboratory, an experimental study reported a peak power output of 355 W at 52.3 km/h (14.53 m/s) (Gonzaléz-Haro et al., 2007). Vogt et al. (2006) assessed in laboratory the averaged power at 11.41m/s in six cyclists and it ranged between 190 W and 392 W. The protocol started with a resistance of 100 W and increments of 20 W each 3 min. The power output was measured in different heart rate zones and near 169 ± 7 bpm power output was 392 ± 55 W. Others assessed the influence of the cycle crank length and presented maximal power values near 1200 W (Martin & Spirduso, 2001). Even more, at 50 km/h (13.89 m/s) power values range between 864 ± 107 W and 940 ± 83 W (Wiles, Coleman, Tegerdine, & Swaine, 2006). Schenau, de Koning & de Groot (1994), reported values of 20 W/Kg in sprinting events between 4 or 5 s. Forte et al. (2020), based on CFD and analytical procedures reported a total mechanical power about 400 W and 2300 W for different positions for 11 and 22 m/s, respectively. Thus, a subject with 55 kg it is expected to deliver a total power near 1100 W. The differences from our study may be due: (i) peak power was measured in laboratory and experimental testing; (ii) the tested speeds were different of our study. The influence of the Pd in the power to overcome the resistive forces ranged from 90% to 96%. Actually, at speeds above 6 m/s, drag represent about 90% of the resistive forces (Candau et al., 1999; di Prampero, 1986; Martin, Gardner, Barras & Martin, 2006; Millet & Candau, 2002).

In road cycling, different positions lead to higher or lower energy cost, due the ACd variations (Ryschon & Stray-Gundersen, 1993). In the present study, different helmet types also influence the ACd and drag. Belli & Hintzy (2002) assessed the energy cost at 150 W in five sessions of 4 min separated by one-min rest on an ergometer bicycle at different pedal rates. The energy cost ranged between 1.11 J/m/kg and 2.39 J/m/kg. In our study, the subject had 55 kg, hence energy cost at 150 W may range between 61.05 J/m and 131.45 J/m. Nevertheless, during the Tour de France, the mean expenditure per day was 25.4±1.40 MJ (Saris, Erp-Baart, Brouns, Westerterp, & Hoor, 1989). In the same study, the mean distance covered per day was 155.59 km. Hence, an energy cost of 163.25 J/m. As far as our understanding goes, the mean speed in Tour de France is near 40 km/h (Lucia et al., 2003; El Helou et al., 2010). These results of energy cost are slightly higher than the results of the present study at the same speed. That can be explained by the methods used to assess or estimate the energy expenditure. Saris et al. (1989), estimated the energy expenditure of all the daily activities, including the race, recovery and resting time. The energy cost was estimated for the entire day; whereas, in the current study the energy cost was measured per unit of distance travelled during the race or stage. To assess the energy cost, a gross efficiency of 20% was defined. That was supported by literature where gross efficiency ranges between 15% and 25% (Bertucci et al., 2012; Ettema & Lorås, 2009). The energy cost varied between 106.89 J/m and 381.40 J/m for booth helmets at the different speeds. At 11.11 m/s, the aero road helmet imposed about 15% less energy cost of transportation; whereas, at 20.83 m/s, the difference between the standard and aero road helmet was 21%. Therefore, at 11.11 m/s, the energy saving between helmets of 155.59 km (mean distance of a stage at the Tour de France) is about 606.15 Kcal (1 Kcal ≈ 4184 J). The ETA with a standard helmet was higher (i.e. would take longer to travel the distance) in comparison to an aero helmet. The subject would have to deliver 327 W to reach 11.11 m/s; whereas with an aero helmet just 290 W. At 20.83 m/s, the subjects would need to impose higher power with a standard helmet (1614.35 W) in comparison to an aero helmet (1334.15 W). Overall, in a stage of 152 km, at 327 W and 1614.35 W, a cyclist wearing an aero helmet may save 1543.41 and 1265.42 s in comparison to a standard helmet. The standard helmet imposes higher drag than the aero helmet, thus for the same mechanical power, the cyclist may reach higher speeds wearing the latter type. Even more, time-trial helmets and similar to these, seem to impose less drag in comparison to standard helmets (Sidelko, 2009; Forte et al., 2016; Forte et al; 2017).

Based on this methodology, coaches should advise their athletes to use aero road helmets during a race (namely in races and/or stages without uphill and downhill events) due to their similarities with the time-trial helmets. Athletes may also adopt the elbows position as much as possible using aero road helmets to minimize the resistive forces. This allows them to minimize drag, the required mechanical power and energy cost. This methodology may help coaches to prescribe training intensities for the required muscular power at a given speed or pace. This knowledge may allow improving the cyclist's muscular power and increasing the aerobic power. Even more, manufacturers may design and produce new helmets considering the time-trial models, improving the comfort and (minimizing) the air vents.
This study presents the following limitations: (i) the subject is only representative of an elite cohort of cyclists; (ii) only one position was assessed and compared; (ii) only two helmets were evaluated; (iii) a set of assumptions were used to estimate the resistive forces (rolling resistance coefficient, temperature, air density and gross efficiency); This study is a static analysis and dynamic measures may differ.

5. Conclusions

The resistance action upon a cyclist in a time-trial position wearing a standard and aero helmet varies across different speeds. The mechanical power and energy cost seem to increase with speed. The standard helmet demanded more power at the selected speeds. The cyclists, coaches and sports scientists might be aware that the aero helmet imposed less drag. Upon that, with an aero helmet the cyclist will required to deliver less mechanical power in comparison to the standard helmet. Finally, a cyclist wearing the aero helmet, for the same mechanical power, may reach a higher velocity in comparison to the standard helmet.

Acknowledgments: Non-declare

Conflicts of Interest: The authors declare no conflict of interest

References

Aroussi, A., Kucukgokoglan, S., Pickering, S. J., & Menacer, M. (2001). Evaluation of four turbulence models in the interaction of multi burners swirling flows. In Proceedings of the 4th International Conference on Multiphase Flow, New Orleans, LA, USA, 27th May–1st June 2001.

Barbosa, T. M., Forte, P., Estrela, J. E., & Coelho, E. (2016). Analysis of the Aerodynamics by Experimental Testing of an Elite Wheelchair Sprinter. Procedia Engineering, 147, 2–6.

Barelle, C., Chabroux, V., & Favier, D. (2010). Modelling of the time trial cyclist projected frontal area incorporating anthropometric, postural and helmet characteristics. Sports Engineering, 12(4), 199–206.

Beaumont, F., Taiar, R., Polidori, G., Trenchard, H., & Grappe, F. (2018). Aerodynamic study of time-trial helmets in cycling racing using CFD analysis. Journal of Biomechanics, 67, 1–8.

Bertucci, W. M., Betik, A. C., Duc, S., & Grappe, F. (2012). Gross efficiency and cycling economy are higher in the field as compared with on an Axiom stationary ergometer. Journal of Applied Biomechanics, 28(6), 636–644.

Blocken, B., Defraeye, T., Koninckx, E., Carmeliet, J., & Hespel, P. (2013). CFD simulations of the aerodynamic drag of two drafting cyclists. Computers & Fluids, 71, 435–445.

Blocken, B., van Druenen, T., Toparlar, Y., Malizia, F., Mannion, P., Andrianne, T., … Diepens, J. (2018). Aerodynamic drag in cycling pelotons: New insights by CFD simulation and wind tunnel testing. Journal of Wind Engineering and Industrial Aerodynamics, 179, 319–337.

Blocken, B., van Druenen, T., Toparlar, Y., & Andrianne, T. (2018b). Aerodynamic analysis of different cyclist hill descent positions. Journal of Wind Engineering and Industrial Aerodynamics, 181, 27-45.

Brühwiler, P. A., Buyan, M., Huber, R., Bogerd, C. P., Sznitman, J., Graf, S. F., & Rösgen, T. (2006). Heat transfer variations of bicycle helmets. Journal of Sports Sciences, 24(9), 999–1011.

Burke, E. (2003). High-tech Cycling. Human Kinetics. Champaing, IL.

Candau, R. B., Grappe, F., Menard, M., Barbier, B., Millet, G. Y., Hoffman, M. D., Rouillon, J. D. (1999). Simplified deceleration method for assessment of resistive forces in cycling. Medicine and Science in Sports and Exercise, 31(10), 1441–1447.

Chowdhury, H. (2012). Aerodynamic design of sports garments. Applied aerodynamics, 21-40. Lerner, J. C. & Boldes, U. (Ed.), IntechOpen, Rijeka, Croatia.

Debraux, P., Grappe, F., Manolova, A. V., & Bertucci, W. (2011). Aerodynamic drag in cycling: methods of assessment. Sports Biomechanics, 10(3), 197–218.

Defraeye, T., Blocken, B., Koninckx, E., Hespel, P., & Carmeliet, J. (2010a). Aerodynamic study of different cyclist positions: CFD analysis and full-scale wind-tunnel tests. Journal of Biomechanics, 43(7), 1262–1268.

Defraeye, T., Blocken, B., Koninckx, E., Hespel, P., & Carmeliet, J. (2010b). Computational fluid dynamics analysis of cyclist aerodynamics: Performance of different turbulence-modelling and boundary-layer modelling approaches. Journal of Biomechanics, 43(12), 2281–2287.

di Prampero, P. E. (1986). The energy cost of human locomotion on land and in water. International Journal of Sports Medicine, 7(2), 55–72.

Dorel, S., Hautier, C. A., Rambaud, O., Rouffet, D., Praagh, E. V., Lacour, J.-R., & Bourdin, M. (2005). Torque and Power-Velocity Relationships in Cycling: Relevance to Track Sprint Performance in World-Class Cyclists. International Journal of Sports Medicine, 26(9), 739–746.

Edwards, A. G., & Byrnes, W. C. (2007). Aerodynamic characteristics as determinants of the drafting effect in cycling. Medicine and Science in Sports and Exercise, 39(1), 170–176.

El Helou, N., Berthelot, G., Thibault, V., Tafflet, M., Nassif, H., Campion, F., Toussaint, J.F. (2010). Tour de France, Giro, Vuelta, and classic European races show a unique progression of road cycling speed in the last 20 years. Journal of Sports Sciences, 28(7), 789–796.

Ettema, G., & Lorås, H. W. (2009). Efficiency in cycling: a review. European Journal of Applied Physiology, 106(1), 1–14.

Faria, E. W., Parker, D. L., & Faria, I. E. (2005). The science of cycling: factors affecting performance - part 2. Sports Medicine, 35(4), 313–337.

Forte, P., Marinho, D. A., Morouço, P. G., & Barbosa, T. (2016). CFD analysis of head and helmet aerodynamic drag to wheelchair racing. 2016 1st International Conference on Technology and Innovation in Sports, Health and Wellbeing (TISHW), 1–6.

Forte, P., Marinho, D. A., Morouço, P., Pascoal-Faria, P., & Barbosa, T. M. (2017). Comparison by computer fluid dynamics of the drag force acting upon two helmets for wheelchair racers. AIP Conference Proceedings, 1863(1), 520005.

Forte, Pedro., Barbosa, T. M., & Marinho, D. A. (2015). Technologic Appliance and Performance Concerns in Wheelchair Racing – Helping Paralympic Athletes to Excel. New Perspectives in Fluid Dynamics, 101–121. Chaoqun Liu (Ed.), IntechOpen, Rijeka, Croatia.

Forte, Pedro, Marinho, D. A., Morais, J. E., Morouço, P. G., & Barbosa, T. M. (2018a). The variations on the aerodynamics of a world-ranked wheelchair sprinter in the key-moments of the stroke cycle: A numerical simulation analysis. PLOS ONE, 13(2), e0193658.

Forte, P., Marinho, D. A., Morais, J. E., Morouço, P. G., & Barbosa, T. M. (2018b). Estimation of mechanical power and energy cost in elite wheelchair racing by analytical procedures and numerical simulations. Computer Methods in Biomechanics and Biomedical Engineering, 21(10), 585-592.

Forte, P., Marinho, D. A., Barbosa, T. M., Morouço, P., & Morais, J. E. (2020). Estimation of an elite road cyclist performance in different positions based on numerical simulations and analytical procedures. Frontiers in bioengineering and biotechnology, 8, 538.

García-López, J., Rodríguez-Marroyo, J. A., Juneau, C.-E., Peleteiro, J., Martínez, A. C., &

Villa, J. G. (2008). Reference values and improvement of aerodynamic drag in professional cyclists. Journal of Sports Sciences, 26(3), 277–286.

González-Haro, C., Ballarini, P. A. G., Soria, M., Drobnic, F., & Escanero, J. F. (2007). Comparison of nine theoretical models for estimating the mechanical power output in cycling. British Journal of Sports Medicine, 41(8), 506–509.

Grappe, F., Candau, R., Barbier, B., Hoffman, M. D., Belli, A., & Rouillon, J.D. (1999). Influence of tyre pressure and vertical load on coefficient of rolling resistance and simulated cycling performance. Ergonomics, 42(10), 1361–1371.

Grappe, F., Candau, R., Belli, A., & Rouillon, J. D. (1997). Aerodynamic drag in field cycling with special reference to the Obree's position. Ergonomics, 40(12), 1299–1311.

Gross, A. C., Kyle, C. R., & Malewicki, D. J. (1983). The Aerodynamics of Human-powered Land Vehicles. Scientific American, 249(6), 142–153.

Kennedy, M. D., & Lampe, W. N. (2013). Applied Ergonomics of Cycling Performance. Handbook of Ergonomics in Sport and Exercise, 115-127. Youlian Hong (Ed.). Routledge, Abingdon, UK.

Kulfan, B. (2000). Assessment of CFD predictions of viscous drag. Fluids 2000 Conference and Exhibit, 2391. Drive, A. B (Ed.). American Institute of Aeronautics and Astronautics, Denver, CO, U.S.A.

Kyle, C. R., & Burke, E. (1984). Improving the racing bicycle. Mechanical engineering, 106(9), 34–45.

Lucia, A., Earnest, C., & Arribas, C. (2003). The Tour de France: a physiological review. Scandinavian Journal of Medicine & Science in Sports, 13(5), 275–283. https://doi.org/10.1034/j.1600-0838.2003.00345.x

Lukes, R. A., Chin, S. B., & Haake, S. J. (2005). The understanding and development of cycling aerodynamics. Sports Engineering, 8(2), 59–74.

Belli, A., & Hintzy, F. (2002). Influence of pedalling rate on the energy cost of cycling in humans. European journal of applied physiology, 88(1-2), 158-162.

Martin, J. C., & Spirduso, W. W. (2001). Determinants of maximal cycling power: crank length, pedaling rate and pedal speed. European Journal of Applied Physiology, 84, 413–418.

Martin, James C., Gardner, A. S., Barras, M., & Martin, D. T. (2006). Modeling sprint cycling using field-derived parameters and forward integration. Medicine and Science in Sports and Exercise, 38(3), 592–597.

Martin, J. C., Milliken, D. L., Cobb, J. E., McFadden, K. L., and Coggan, A. R. (1998). Validation of a mathematical model for road cycling power. J. Appl. Biomech. 14(3), 276-291.

Millet, G. P., & Candau, R. (2002). Facteurs mécaniques du coût énergétique dans trois locomotions humaines. Science & Sports, 17(4), 166–176.

Proctor, T. D., & Rowland, F. J. (1986). Development of standards for industrial safety helmets - The state of the art. Journal of Occupational Accidents, 8(3), 181–191.

Ryschon, T. W., & Stray-Gundersen, J. (1993). The effect of tyre pressure on the economy of cycling. Ergonomics, 36(6), 661–666.

Saris, W. H. M., Erp-Baart, M. A. van, Brouns, F., Westerterp, K. R., & Hoor, F. ten. (1989). Study on Food Intake and Energy Expenditure During Extreme Sustained Exercise: The Tour de France. International Journal of Sports Medicine, 10(S 1), S26–S31.

Schlichting, H., & Gersten, K. (2016). Boundary-Layer Theory. Springer, Berlin, Germany.

Wiles, J. D., Coleman, D., Tegerdine, M., & Swaine, I. L. (2006). The effects of caffeine ingestion on performance time, speed and power during a laboratory-based 1 km cycling time-trial. Journal of Sports Sciences, 24(11), 1165–1171.

Vogt, S., Heinrich, L., Schumacher, Y. O., Blum, A., Roecker, K., Dickhuth, H. H., & Schmid, A. (2006). Power output during stage racing in professional road cycling. Medicine and science in sports and exercise, 38(1), 147.

Zdravkovic, M. M., Ashcroft, M. W., Chisholm, S. J., & Hicks, N. (1996). Effect of cyclist's posture and vicinity of another cyclist on aerodynamic drag. The engineering of sport, 1, 21–28.

Sidelko, S. (2009). Benchmark of aerodynamic cycling helmets using a refined wind tunnel test protocol for helmet drag research. Doctoral dissertation, Massachusetts Institute of Technology, 2007.

van Schenau, G. J. I., de Koning, J. J., & de Groot, G. (1994). Optimisation of sprinting performance in running, cycling and speed skating. Sports Medicine, 17(4), 259-275.

Blocken, B., van Druenen, T., Toparlar, Y., & Andrianne, T. (2018b). Aerodynamic analysis of different cyclist hill descent positions. Journal of Wind Engineering and Industrial Aerodynamics, 181, 27-45.